Conf-931121--27

UCRL-JC-115418
PREPRINT

Fully Coupled Nonlinear Thermomechanical Analysis Including General Contact in PALM2D

Bruce E. Engelmann
Robert G. Whirley

This paper was prepared for submittal to the American Society of Mechanical Engineers Winter Annual Meeting, New Orleans, LA, November 28 - December 3, 1993

October 7, 1993

Fully Coupled Nonlinear Thermomechanical Analysis Including General Contact in PALM2D

Bruce E. Engelmann
Robert G. Whirley

Methods Development Group, L-122
University of California
Lawrence Livermore National Laboratory
P.O. Box 808
Livermore, California 94550

ABSTRACT

Fully coupled thermomechanical analysis solves the thermal problem on the deforming geometry and incorporates thermal loads into the mechanical problem. In contrast, traditional thermal stress analysis is based on an uncoupled approach in which the thermal problem is solved on a fixed geometry, and the resulting temperatures are then used to load a mechanical problem. Thermal contact, in which heat flow paths depend on the mechanical deformations of adjacent surfaces, is a major component of many fully coupled thermomechanical analyses. This paper presents the development of a thermomechanical finite element formulation, including contact. The proposed approach accommodates arbitrarily large relative motions of contact surfaces, fully unstructured meshes, pressure-dependent contact resistance, conduction across small gaps, and approximate models for convection and radiation. The theory described herein has been implemented in the Lawrence Livermore National Laboratory public code PALM2D and has been used to solve a diverse set of thermomechanical problems. Examples illustrating the performance of this code on large deformation thermomechanical problems are presented and discussed.

1. INTRODUCTION

Coupled thermomechanical effects arise in many physical problems where mechanical deformation generates heat, where deformations are large, or where multiple bodies come into contact and exchange heat across the interface. These problems are fully coupled, in contrast to the classical thermal stress problem where the temperature field drives the mechanical response but the mechanical response has no effect on the thermal problem. Although numerical methods for the classical thermal stress problem have received much attention over the years, much less consideration has been given to the fully coupled problem. Further, the computational treatment of general thermomechanical contact conditions in a finite element context has similarly received little attention. This paper discusses an efficient nonlinear finite element method for the fully coupled thermomechanical problem, and highlights the development of a general thermomechanical contact capability and fully adaptive solution algorithm.

Fully coupled thermomechanical problems arise in many areas of engineering. For example, in the analysis of explosives containers subjected to fire environments, deformations may be sufficiently large that they affect the solution to the heat transfer problem, thus requiring a coupled solution for accurate results. Similarly, the simulation of metal forming manufacturing operations frequently requires the ability to include heat generation by mechanical deformation and thermomechanical contact effects in the analysis. For example, in the extrusion of metal parts, the large plastic deformations can generate enough heat to cause thermal softening of the material, and evolving thermomechanical contact affects the cooling of the workpiece through heat transfer to the die. These effects combine to produce temperature gradients in the workpiece which strongly affect subsequent deformation patterns. Such metal forming process simulations allow production operations to be optimized, and therefore reduce waste and cost. These examples illustrate some of the diverse problem areas which require a fully coupled thermomechanical analysis.

The objective of this research was to develop a powerful thermomechanical contact capability and an adaptive solution methodology for the solution of fully coupled thermomechanical problems. In addition, it was desirable to develop a numerical method which was highly vectorizable to yield good performance using modern supercomputers on real engineering analysis problems.

The outgrowths of this research have been implemented into the Lawrence Livermore National Laboratory (LLNL) coupled thermomechanical code PALM2D (Engelmann, Whirley, and Shapiro, 1990). The initial version of PALM2D introduced an implementation of the staggered step formulation which integrates portions of the LLNL NIKE2D (Engelmann and Hallquist, 1991) and TOPAZ2D (Shapiro and Edwards, 1990) codes to solve the fully

coupled thermomechanical problem. The work described herein has substantially extended the capabilities of PALM2D beyond those of the initial version and has allowed the solution of new classes of interesting problems.

2. FORMULATION

This section describes the formulation of the proposed adaptive staggered step approach to coupled thermomechanical analysis with contact First, the governing equations are stated and the appropriate boundary conditions are given, highlighting the statement of thermomechanical contact conditions. The development of semidiscrete matrix equations is then briefly outlined for both the energy equation and the momentum equation. Next, a brief summary of algorithms for the adaptive solution of the nonlinear algebraic equations is presented. Finally, the coupling methodology and its implementation is discussed in some detail.

2.1 The Energy Equation

For an anisotropic solid, the energy equation on a continuum domain Ω may be written

$$(k_{ij}T_{,j})_{,i} + Q^T + Q^M = \rho c\dot{T}, \tag{1}$$

where T is temperature, k_{ij} is the thermal conductivity tensor, Q^T is the volumetric rate of heat generation from thermal sources, Q^M is the volumetric rate of heat generation from mechanical sources, ρ is the material density, and c is the heat capacity.

The solid has a boundary Γ which can be divided into a boundary Γ_{TT} where temperatures are prescribed, a boundary Γ_{TF} where heat flux is prescribed, and a boundary Γ_{TC} where flux conditions such as convection, radiation, and interface conduction depend on the position of the body relative to other bodies.

Conditions on Γ_{TT} and Γ_{TF} may be written as:

Specified Temperature.

$$T = T^s(\boldsymbol{x}, t) \text{ on } \Gamma_{TT}, \tag{2}$$

where T^s is a *given* function, $\boldsymbol{x}$ is a position vector in Ω, and t is time, or

Specified Surface Heat Flux.

$$q_i n_i = -q^s(\boldsymbol{x}, t) \text{ on } \Gamma_{TF}, \tag{3}$$

where q^s is a *given* function, q_i are components of the heat flux vector, and n_i are components of the outward surface normal vector.

Conditions on Γ_{TC} may be written as the sum of several heat flux contributions,

$$q_i n_i = q_{CF} + q_{CI} + q_{RI} + q_{RF}, \tag{4}$$

where q_{CF} is the heat flux due to natural or forced convection, q_{CI} is the heat flux due to interface conduction, q_{RI} is the heat flux due to interface radiation, and q_{RF} is the heat flux due to far-field radiation. The boundary conditions on Γ_{TC} are schematically depicted in Figure 1.

Convection.

$$q_{CF} = h_{CF}(T - T_e) \text{ on } \Gamma_{TC}, \tag{5}$$

where h_{CF} is the convective heat transfer coefficient and T_e is the free-stream temperature. Motivated by the discussion in (Welty, Wicks, and Wilson, 1976), the specific form of h_{CF} has been chosen to be

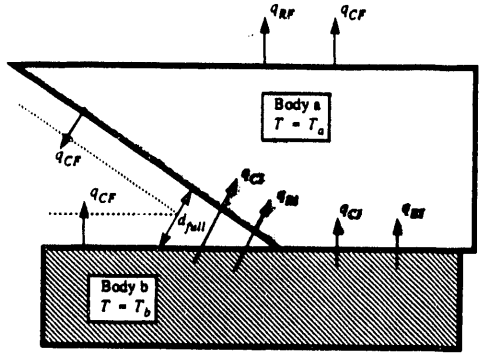

Figure 1: Schematic depiction of the thermal boundary conditions.

$$h_{CF} = \kappa(g_N)\bar{h}_{CF}(\boldsymbol{x}, t, T)(T - T_e)^{\alpha}, \tag{6}$$

which can characterize various types of free convection for nonzero exponents α. Multiplier $\kappa(g_N)$ has the effect of stopping or slowing convective heat transfer when adjacent bodies come close or touch and thereby inhibit the convective transfer process. The function $\kappa(g_N)$ is defined as

$$\kappa(g_N) = \begin{cases} 1 & \text{if } g_N \geq d_{full} \\ \frac{(g_N - d_{full})}{(d_{full} - d_{cut})} & \text{if } d_{cut} < g_N < d_{full} \\ 0 & \text{if } g_N \leq d_{cut}, \end{cases} \tag{7}$$

where d_{full} and d_{cut} are empirically determined distances. Thus, when another body approaches Γ_{TC} closer than d_{cut}, then it is assumed that boundary layer interaction prevents significant convective fluid motion and the convective flux is set to zero. When an approaching body is farther away than d_{full}, then boundary layer interaction is assumed negligible and the full convective heat flux is used in the computation. For approach distances between d_{full} and d_{cut}, a linear interpolation is used as represented in (7).

vspace.25in

Interface Conduction.

$$q_{CI} = h_{CI}(T_a - T_b) \text{ on } \Gamma_{TC}, \tag{8}$$

where T_a and T_b represent the surface temperature of body a and body b, respectively. The specific form of conductance h_{CI} depends on whether two adjacent bodies are in contact. When bodies are in contact ($t_N < 0$), the conductance h_{CI} is an empirically based function of contact pressure and temperature,

$$h_{CI} = h_{CI}(t_N, T), \tag{9}$$

and depends on such things as material properties and the shape and distribution of surface asperties (i.e., surface roughness). When

two adjacent bodies are not in contact ($t_N = 0$), but are close to one another, heat is (potentially) conducted across the interface through the medium filling the gap and thus

$$h_{CI} = h_{CI}(g_N, t). \tag{10}$$

Generally, conductance across the interface will diminish as the bodies move away from one another, perhaps dropping off as $\frac{1}{g_N}$ in simple cases.

Interface Radiation.

$$q_{RI} = h_{RI}(g_N, T)(T_a^4 - T_b^4) \text{ on } \Gamma_{TC}, \tag{11}$$

where h_{RI} is the interface radiation coefficent. Radiative heat transfer takes place between surfaces of adjacent bodies. When bodies are close together, coefficient h_{RI} can be determined based on the same considerations as radiation between two parallel planes.

Far Field Radiation.

$$q_{RF} = h_{RF}(\boldsymbol{x}, T, t)(T_a^4 - T_\infty^4) \text{ on } \Gamma_{TC}, \tag{12}$$

where h_{RF} is the far-field radiation coefficient which may be a function of position, time, or temperature, and T_∞ is the exchange body temperature. The coefficient h_{RF} characterizes the effect of geometric view factor, emissivity, and reflectivity on the amount of radiative heat transfer between boundary Γ_{TC} and a far away body.

In order to properly handle the case where one body is initially close to another body so that interface radiation dominates, and subsequently moves far away so that far field radiation dominates at a later time, a linear interpolation from q_{RI} to q_{RF} based on distance g_N is postulated. The interface (near-body) radiative mechanism is considered dominant when two bodies are closer than a given distance d_{near}, the far-field radiative mechanism is considered dominant when two bodies are farther apart than a given distance d_{far}. In an analogous way to that described above for convection, linear interpolation based on the distance g_N is used to find the radiative heat flux contribution for $d_{near} < g_N < d_{far}$

In addition, for transient problems, temperature initial conditions of the form

$$T(\boldsymbol{x}, 0) = T_0(\boldsymbol{x}) \; \forall \boldsymbol{x} \in \Omega \tag{13}$$

must be specified.

2.2 The Momentum Equation

The continuum equations of motion on a domain Ω may be written

$$\sigma_{ij,j} + b_i = \rho \ddot{u}_i, \tag{14}$$

where σ_{ij} is the Cauchy stress tensor, b_i is the body force density per unit volume, ρ is the mass density, and u_i are the displacements. Superimposed dots denote differentiation with respect to time, lower-case indices are assumed to range from one to three, and repeated indices are summed.

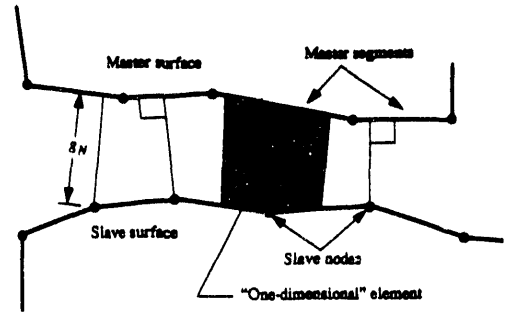

Figure 2: Discretization of the contact boundary showing the gap function g_N, the "effective one-dimensional conduction element," and the interface element area A.

The continuum boundary Γ can be divided into a boundary Γ_{MU} where displacements are prescribed, a boundary Γ_{MT} where surface tractions are prescribed, and a boundary Γ_{MC} where mechanical contact conditions apply. Conditions on the boundary may be written as

$$u_i = u_i^g(\boldsymbol{x}, t) \text{ on } \Gamma_{MU}, \tag{15}$$

where u_i^g is a *given* function, or

$$\sigma_{ij} n_j = t_i^g(\boldsymbol{x}, t) \text{ on } \Gamma_{MT}, \tag{16}$$

where $t_i^g(\boldsymbol{x}, t)$ is a *given* function and n_i denotes the outward surface normal vector, or

$$\sigma_{ij} n_i n_j = t_N(\boldsymbol{x}) \text{ on } \Gamma_{MC}, \tag{17}$$

where t_N is the normal surface traction (negative in compression) arising from the contact of two bodies. To define the mechanical conditions on Γ_{MC}, it is convenient to introduce a gap function g_N which is the "distance" between a point on one body and its closest point projection on another, as shown in Figure 2. The mechanical contact conditions can then be written

$$t_N(\boldsymbol{x}) \leq 0, \tag{18}$$

$$g_N(\boldsymbol{x}) \geq 0, \tag{19}$$

$$t_N(\boldsymbol{x}) g_N(\boldsymbol{x}) = 0. \tag{20}$$

Thus, the normal traction t_N is nonzero only when the gap g_N is zero, and conversely, the gap g_N is greater than zero only when the normal traction t_N is zero.

In addition, initial conditions on velocity

$$\dot{u}_i(\boldsymbol{x}, 0) = \dot{u}_0(\boldsymbol{x}) \; \forall \boldsymbol{x} \in \Omega \tag{21}$$

must be specified for dynamic problems.

2.3 Matrix Equations

The weak forms of the momentum equation and the energy equation are constructed separately using standard techniques. After introducing a spatial finite element discretization this results in a set of second order and first order nonlinear ordinary differential equations in time. This process is briefly outlined below.

Energy Equation. Constructing the weak form of the energy equation (1), using boundary conditions (2) - (4), and using a finite element spatial discretization yields a coupled system of first order ODEs of the form

$$\boldsymbol{C}\dot{\boldsymbol{T}} + \boldsymbol{G}^{int}(\boldsymbol{T}) = \boldsymbol{R}(\boldsymbol{T}, \boldsymbol{Q}^T, \boldsymbol{Q}^M, t), \tag{22}$$

where $\boldsymbol{C}$ is a capacitance matrix, $\boldsymbol{T}$ is a vector of nodal temperatures, $\boldsymbol{G}$ is a vector of internal nodal heat fluxes, $\boldsymbol{R}$ is a vector of external nodal heat fluxes which also includes contributions from internal heat generation, $\boldsymbol{Q}^T$ is a vector of element thermal heat generation rates, and $\boldsymbol{Q}^M$ is a vector of element mechanical heat generation rates.

If steady-state conditions are assumed, then $\dot{\boldsymbol{T}} = 0$ in (22) and a nonlinear algebraic equation is obtained. This equation is then solved using an incremental approach described in the following section. If transient thermal effects are considered, the ODEs (22) are discretized in time using the midpoint rule, again yielding a nonlinear algebraic system to be solved at each time step.

Momentum Equation. Constructing the weak form of the momentum equation (14), using boundary conditions (15) - (17), and spatially discretizing the resulting equations using finite elements yields a coupled system of second order ODEs of the form

$$\boldsymbol{M}\ddot{\mathbf{u}} + \boldsymbol{F}^{int}(\mathbf{u}, \dot{\mathbf{u}}, \boldsymbol{T}) = \boldsymbol{P}(\mathbf{u}, \mathbf{b}, t, \mathbf{T}), \tag{23}$$

where $\boldsymbol{M}$ is a mass matrix, $\boldsymbol{F}^{int}$ is an internal nodal force vector, $\boldsymbol{P}$ is an external nodal force vector, $\mathbf{u}$ is a vector of nodal displacements, and $\boldsymbol{T}$ is a vector of nodal temperatures.

Note that, in general, both the internal nodal force vector $\boldsymbol{F}^{int}$ and the external nodal force vector $\boldsymbol{P}^{ext}$ are functions of temperature $\boldsymbol{T}$. In addition, the external nodal force vector $\boldsymbol{P}$ contains contributions from mechanical boundary conditions and loads as well as from contact pressure arising from the contact of two or more bodies.

For "quasistatic" analysis, $\ddot{\mathbf{u}} = 0$ in (23), but the equations may still be time-dependent if viscous effects are incorporated into $\boldsymbol{F}^{int}$, such as from a rate-dependent constitutive equation. For the special case where $\boldsymbol{F}^{int}$ is not explicitly time-dependent, then (23) is a set of nonlinear algebraic equations to be solved at each load step of an incremental approach. For time-dependent analysis, (23) may be discretized in time using the Newmark-β time integration scheme. This results in a similar set of nonlinear algebraic equations which must be solved at each time or load step.

2.4 Thermomechanical Contact

The contact algorithms presented herein are based on a slave node on master segment concept. Search algorithms are used to find the closest point projection of a slave node onto a master segment, as shown in Figure 2.

The external nodal forces arising from mechanical contact are derived using a penalty or augmented Lagrangian approach for the enforcement of the inequality constraints (18)-(20). The details of this procedure are discussed in (Laursen, 1992) and are not repeated here.

The nodal heat fluxes arising from thermal contact are found by assuming one-dimensional heat conduction between the slave node and the closest point on the master segment in a manner similar to that discussed in the excellent paper, (Zavarise, Wriggers, Stein, and Schr fler, 1992). An average tributary area A, shown in Figure 2, is computed for the slave and master node pair and is used to compute the total heat flux across the contact surface. Some care must be used in the computation of this average area for the case in which one or both sides of the interface is sharply curved.

2.5 Solution Algorithms and Coupling

A "staggered step" approach is used to achieve the thermomechanical coupling in an efficient and versatile setting for use with adaptive solution methods. In this approach, thermal calculations are performed on the geometry calculated at the end of the previous step. The resulting temperature field is then used in the mechanical calculations to find the updated geometry and stress fields. The thermal problem and the mechanical problem are each solved using an implicit formulation, although an explicit formulation could be used for either component with only minor changes to the coupling algorithm. At each time step, a set of nonlinear algebraic equations is generated for the thermal problem, and another set is generated for the mechanical problem. These two systems of nonlinear equations are individually solved using a linearization and iteration procedure.

The alternative to the staggered step formulation is a fully implicit coupling, wherein all thermal and mechanical unknowns are assembled into one large, nonlinear algebraic system of equations. These equations are then solved simultaneously for the updated thermal and mechanical response variables. The fully implicit formulation enjoys more robust time stability properties than does the staggered step formulation, but requires substantially more computer memory and execution time, and is somewhat less flexible with adaptive methods. Further, time stability has not been observed to be a difficulty for the engineering problems studied thus far, and the technology for fully implicit coupling may not exist for some coupled thermomechanical-chemical problems of interest.

It is often desirable to use different step sizes in the thermal and mechanical solution procedures due to differing physical time constants. For example, during a phase change the thermal properties of a material may evolve very rapidly, and thus a very small thermal time step must be used. It is often possible to use a much larger mechanical step size and still obtain an accurate solution to these problems. Conversely, a large deformation problem may require relatively small mechanical steps while tolerating quite large thermal steps in achieving a solution. The staggered step approach facilitates "substepping" within either the thermal or mechanical step to accommodate these problems. Frequently, these regimes are intermingled and occur during different stages of the same problem. It is therefore highly desirable to have an adaptive solution methodology which can automatically adjust the thermal and mechanical step sizes, based on given criteria, to obtain a solution.

The staggered step formulation in PALM2D is interfaced with the adaptive solution control language ISLAND (Engelmann and Whirley, 1991) to incorporate adaptive time steps and solution procedures for the thermal and mechanical problems. ISLAND, Interactive Solution Language for an Adaptive Nike Driver, is a solution control language which allows the flexible specification of adaptive solution procedures. Adaptivity may be based on evolving solution quantities such as incremental change in temperature, strains, or strain rates, or on past iteration convergence behavior.

ISLAND in PALM2D may change the time step size for either the thermal or mechanical problem, may alter the iterative solution algorithm, or may back up (in solution time) in case of nonconvergence and retry the next step with altered solution control parameters. ISLAND in PALM2D can also be used to control boundary conditions and loads based on the evolving solution. This capability can be used to solve coupled thermomechanical problems subjected to external constraints, such as maintaining target strainrates in a superplastic forming problems.

2.6 Implementation

This section briefly outlines the solution procedures as implemented in PALM2D. In the following, subscripts refer to time step number, and it is assumed for simplicity that substepping is not used. The extension of these ideas to accommodate substepping is straightforward but notationally intensive.

For both the steady state and transient cases, the nonlinear algebraic system for the thermal problem arising from (22) is solved by an incremental Newton-Raphson iteration procedure to find the nodal temperature vector $\boldsymbol{T}_{n+1}$ assuming that all quantities at time t_n are known. During this solution procedure, all spatial integrals and derivatives in (22) are evaluated on the most recent geometry $\boldsymbol{x}_n$ and incorporate the current mechanical volumetric rate of heat generation $\boldsymbol{Q}_n^M$. The mechanical contact conditions are held constant throughout the thermal step, and therefore the gap parameter appearing in the thermal contact equations is also constant. This assumption facilitates the use of a consistent linearization of the energy equation in the iterative solution process.

Similarly, the nonlinear system for the mechanical problem arising from (23) is solved by a linearization and iteration procedure for the displacement vector $\mathbf{u}_{n+1}$ assuming that all mechanical quantities at time t_n are known and thermal quantities at time t_{n+1} are known. Our experience has indicated that often quasinewton methods, such as BFGS, offer cost-effective solutions to (23). A complete discussion of the nonlinear solution procedures in PALM2D and NIKE2D is given in (Engelmann and Whirley, 1991) and their implementation is discussed in (Whirley and Engelmann, 1991).

3. APPLICATIONS

The new version of the LLNL public code PALM2D described herein has been used to solve a variety of coupled problems at LLNL.

3.1 Thermal Contact Example

In order to illustrate the behavior of the various thermal contact boundary conditions in a simple context, the two body thermomechanical problem shown in Figure 3 was solved with PALM2D. Th top and bottom three inch square blocks are given initial temperatures of 1000° and 0°, respectively, and the temperature of the gas in the gap region is 200°. The temperature of the bottom surface of the bottom block is prescribed to be 0°, and the temperature of the top surface of the top block is prescribed to be 1000°. The sides of the blocks are insulated. Initially separated by a two inch gap, the blocks are first moved into contact, and then pressed into one another. Next, the top block is slid across the bottom block, while maintaining th contact pressure, until it slips off the bottom block and elastically rebounds.

Figure 4 shows the temperature at several points on the lower block as a function of time. The vertical lines in the figure serve to delineate the various contact regimes. The interface conduction is assumed to be both gap and pressure dependent to illustrate this flexibility. For times between 0 and 2500, the blocks have only convective heat transfer with the gas in the gap region, and reach a thermal equilibrium. Gap conduction becomes active at $t = 2500$ and increases until $t = 10,000$, when the blocks come together. The heat transfer rate into the lower block, and thus its temperature, is increasing during this process. Contact pressure increases between times of 10,000 and 12,500, and further increases the heat transfer rate. Sliding motion occurs from $t = 12,500$ to $t = 15,000$, when the top block slides off of the bottom block. During this sliding, the leftmost part of the bottom block first loses contact with the warmer top block, begins losing heat to the gas by convection, and thus cools first. The middle and right top locations on the bottom block are subsequently exposed, and thus begin the cooldown process at successively later times as shown by the dotted and dashed lines in the figure. The top block remains stationary for $t > 15,000$ and temperatures in the lower block return to thermal equilibrium with the gas, exchanging heat only through convection. This example demonstrates the lower block first attaining thermal equilibrium, next

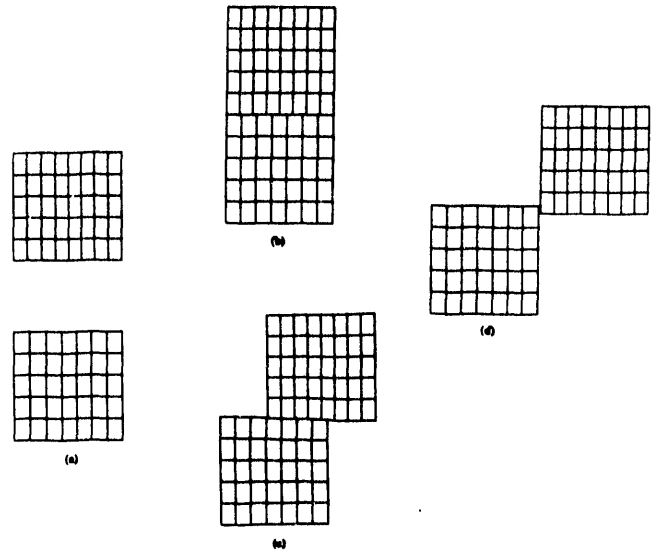

Figure 3: Geometric sequence of motion showing the onset of contact, sliding motion, and separation.

being perturbed from equilibrium by contact with a moving hot block, and finally returning to equilibrium once the hot block has passed.

3.2 Solidification Analysis

The second example is a solidification analysis performed at LLNL. The objective of this simulation was to determine the shrinkage and residual stresses in an aluminum melt as it solidified in a steel can. The axisymmetric finite element model is shown in Figure 5. Mechanical loads arising from gravity were included, as were radiation and convection heat transfer on the top surface of the melt and the outside surface of the can. Thermomechanical

slidelines were defined between the aluminum and steel. Interface conduction was enabled across the slideline with a gap and pressure dependent conductance.

The melt was given an initial temperature of 940° K, slightly above T_{melt} = 933° K. The can cools by exchanging heat with its environment, and the molten aluminum solidifies and shrinks by 6.6% (by volume). This shrinkage causes the aluminum to pull away from the can wall, diminishing further heat transfer across the interface. A time sequence of heat flux vector plots at four stages of the solidification is shown in Figure 6. The early stage plot shows that heat is flowing smoothly from the melt into the can wall all along the boundary since the aluminum is initially in contact. Subsequent figures show the melt solidifying and pulling away from the can wall. Aluminum initially separates from the can wall at the top, and then "unzips" progressively further down the can wall until, at the final stage, contact is retained only in the

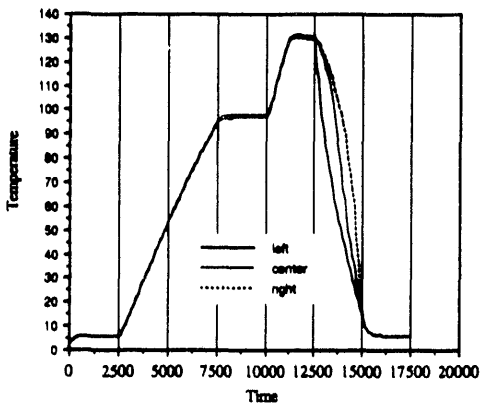

Figure 4: Temperature at left, center, and right top edge of lower block as a function of time. Note the dramatic influence of thermal contact conditions on the temperature variations.

corner region. This simulation is representative of a fully-coupled problem, and the importance of a general thermomechanical contact boundary is clear.

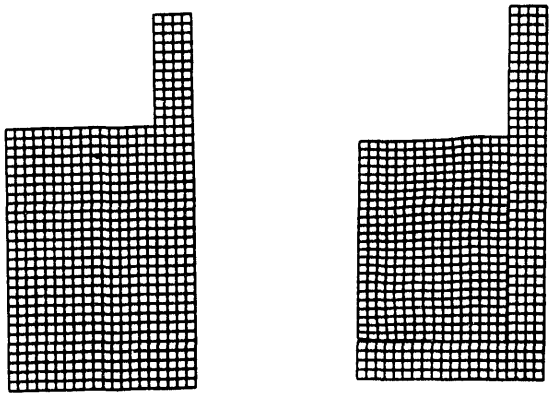

Figure 5: Axisymmetric finite element mesh on the original geometry (left) and the final geometry (right) for the solidification of an aluminum melt in a steel can.

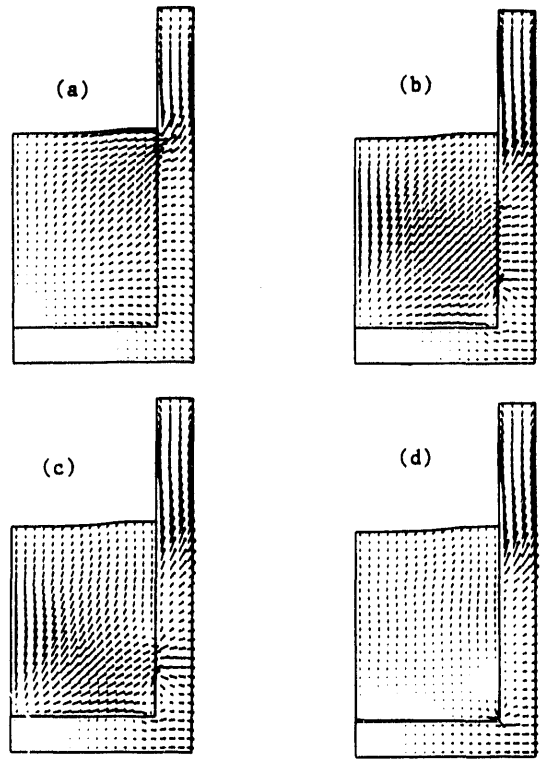

Figure 6: Time sequence of heat flux vectors showing the effect of changing contact conditions on the heat flow path.

4. SUMMARY

This paper has presented a general thermomechanical contact formulation including aspects of pressure and gap dependent interface conduction, convection in gap regions, and interface radiation. The concepts were presented in the context of a staggered step approach for the solution of fully coupled thermomechanical problems. An effective adaptive solution strategy for the resulting equations was outlined and discussed. The thermomechanical contact algorithms and adaptive solution methodologies have been implemented into the LLNL public code PALM2D. The application of PALM2D to a simple slider problem and a solidification problem were discussed to illustrate the performance of the proposed formulation in actual engineering applications.

ACKNOWLEDGEMENTS

The authors wish to acknowledge Drs. Jim Maltby and Peter Raboin of LLNL for numerous helpful and stimulating discussions.

Work performed under the auspices of the U.S. Department of Energy by the Lawrence Livermore National Laboratory under contract W-7405-Eng-48.

REFERENCES

1. Engelmann, B. E., Whirley, R. G., and Shapiro, A. B., 1990, *PALM2D: A Nonlinear Finite Element Program for the Coupled Thermomechanical Response of Solids in Two-*

Dimensions, University of California, Lawrence Livermore National Laboratory, Report UCID-21868.

2. Engelmann, B. E., and Hallquist, J. O., 1991, *NIKE2D - A Nonlinear, Implicit, Two-Dimensional Finite Element Code, User Manual*, University of California, Lawrence Livermore National Laboratory, Report UCRL-MA-105413.

3. Engelmann, B. E., and Whirley, R. G., 1991, *ISLAND: Interactive Solution Language for an Adaptive Nike Driver, User Manual*, University of California, Lawrence Livermore National Laboratory, UCRL Report.

4. Laursen, Tod A., 1992, *Formulation and Treatment of Frictional Contact Problems Using Finite Elements*, Ph. D. Thesis, Stanford University.

5. Shapiro, A. B., and Edwards, A. L., 1990, *TOPAZ2D Heat Transfer Code Users Manual and Thermal Property Data Base*, University of California, Lawrence Livermore National Laboratory, Report UCID-ID-104558.

6. Welty, Wicks, and Wilson, 1976, *Fundamentals of Momentum, Heat, and Mass Transfer*, Second Edition, John Wiley and Sons, New York.

7. Whirley, R. G., and Engelmann, B. E., 1991, *Adaptive Solution Strategies for Nonlinear Finite Element Analysis in Solid Mechanics*, University of California, Lawrence Livermore National Laboratory, Report UCRL-53868-90.

8. Whirley, R. G., and Engelmann, B. E., 1991a, "An Innovative Approach For Coupled Thermomechanical Analysis," ASME Winter Annual Meeting, paper 91-WA-CIE-1.

9. Zavarise, G., Wriggers, P., Stein, E., and Schrefler, B., 1992, "Real Contact Mechanisms and Finite Element Formulation - A Coupled Thermomechanical Approach," *International Journal for Numerical Methods in Engineering*, Vol. 35, pp. 767-785.

END

DATE FILMED

12/9/93